Multi-robot Simultaneous Localization and Mapping based on Pose Graphs Fusion

Guangchuan Yin[a], Zhenping Sun[*] and Wei Wang[b]

College of Intelligent Science and Engineering, National University of Defense Technology, Changsha 410073, China

*Corresponding author e-mail: 13974913933@163.com, [a]17670750976@163.com, [b]13974848663@163.com

Abstract. This paper describes an efficient method for multi-robot simultaneous localization and mapping (SLAM), which establishes a joint model of multi-robot pose graphs based on several special inner and outer loop points called conjunction points. An optimization algorithm based on the fusion of pose graphs is proposed. The rapid fusion of multiple local sub graphs is realized by using the robot encounter information, thus solving the problem of indeterminate positional relationship of the robot and realizing the optimization of the global map.

1. Introduction

The research of multi-robot SLAM is based on the single robot SLAM. The single robot SLAM has enough complexity and it will inevitably add additional challenges when moving to multiple robots platforms [1, 2]. For multi-robot SLAM, scholars have proposed various filtering-based solutions which take advantage of the consistency and accuracy [3]. However, the calculation process is too complicated and it is hard to handle the closure circumstance [4]. Therefore, researchers gradually transferred from the traditional filter optimization algorithm to graph optimization algorithm [5].

In this paper, the idea of conjunction point is proposed based on the existing graph optimization algorithm. The conjunction points are used to transform the respective poses of each pose graph into the global frame. The update of conjunction point replaces the update of the pose graph of the traditional graph optimization algorithm, which simplifies the traditional graph optimization method and improves the speed and accuracy of the global map creation, laying a solid foundation for further multi-robot co-location [6]. The comparison between multi-robot SLAM after introduction of conjunction points and traditional multi-robot SLAM is shown in Figure 1 and Figure 2.

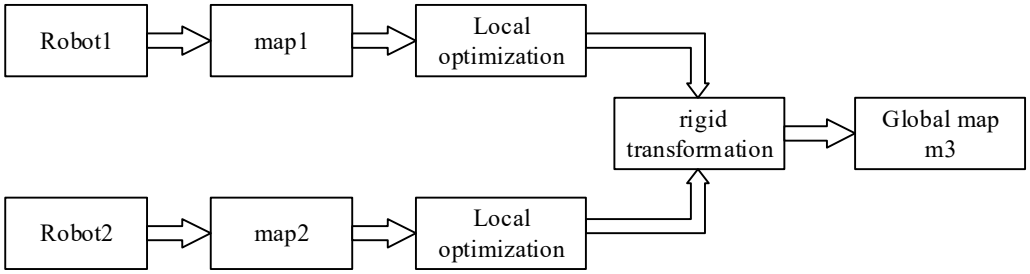

Figure 1. Ordinary multi-robot SLAM process.

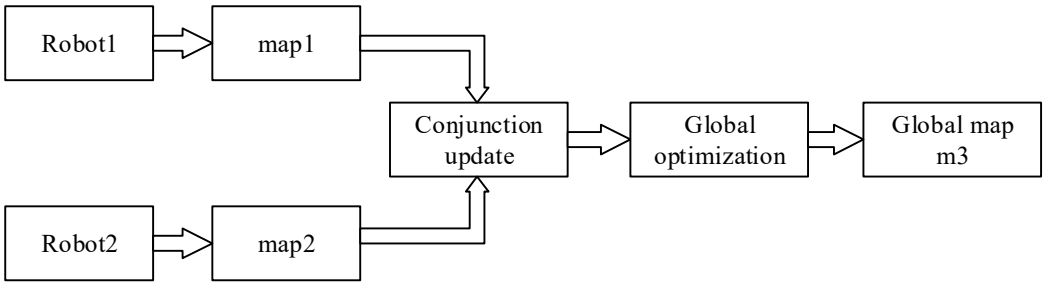

Figure 2. Multi-robot SLAM process after introduction of conjunction points.

2. Approach

2.1. Multi-robot Relative Pose Initialization

Firstly, the multi-robot SLAM problem is represented by the pose graphs of multiple robots in the global coordinate system [7]. A series of factor graphs is used here to describe this process intuitively, in which node represents robot pose and edge represents motion trajectory from one node to another. Figure 3 shows the Markov chain of two robots. The shaded circles represent pose variables and the black dots represent measurements. For R robots, the trajectory $r \in \{1,2,\mathrm{L}\ ,R-1\}$ of robot is given by M_r+1 pose variables $\{x_i^r\}_{i=1}^{M_r+1}$. Then the degree of freedom of each trajectory r is fixed by introducing a prior (generally selecting the coordinate origin) [8]. There are two forms of constraints between poses of a single trajectory: the relationship between successive poses (scan matching results from laser), while the other type of constraint connecting two nearby nodes when loop closing is detected [9]. For the sake of simplicity, the loop closing constraint is omitted in the pose graph, and only the constraints between successive poses are shown in the example of Figure 3.

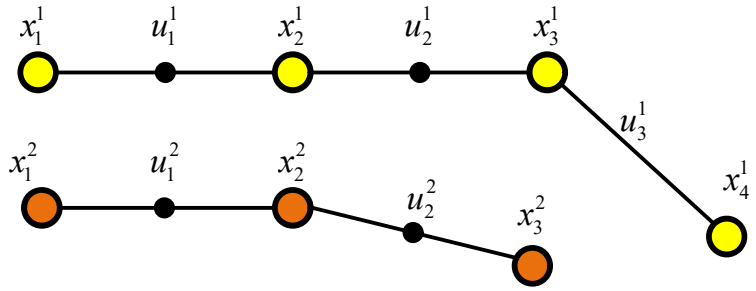

Figure 3. Two pose graphs for two robots without encounters.

The trajectories of the robots described above are completely independent and is now changed by introducing encounters between robots. The encounter e_n between the two robots r and r' is a measurement of connection of the two robots shown in Figure4, highlighted in blue dot t.

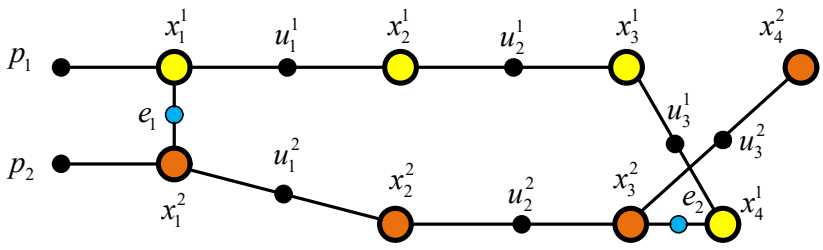

Figure 4. Pose graphs of two robots with two encounters.

This paper applies probabilistic methods to estimate the actual trajectory of the robot based on all measurements [10]. All pose variables $X=\left\{x_i^r\right\}_{r=1,i=1}^{R,M_r+1}$, measurements and priors $Z=\left\{u_i^r\right\}_{r=1,i=1}^{R,M_r+1}\mathrm{U}\left\{p_r\right\}_{r=1}^{R}$ and encounters $E=\left\{e_n\right\}_{n=1}^{N}$ are given by equation (1),

$$P(X,Z,C)\propto\left(P(x_1^r\mid p_r)\prod_{i=2}^{M_r+1}P(x_i^r\mid x_{i-1}^r,u_i)\right)\prod_{n=1}^{N}P(x_{i_n}^{r_n}\mid x_{j_n}^{r'_n},e_n) \tag{1}$$

The process model of laser scan matching is described by equation (2). The noise term w_i^r is a zero-mean Gaussian distribution with covariance matrix Λ_i^r.

$$x_i^r=f_i(x_{i-1}^r,u_i^r)+w_i^r \tag{2}$$

The process model that simulates the encounter between robots is described by equation (3), where the noise term is a zero-mean Gaussian distribution with covariance matrix Γ_n.

$$x_{i_n}^{r_n}=h_n(x_{j_n}^{r'_n},e_n)+v_n \tag{3}$$

Calculating the Maximize a Posterior (MAP) estimate of the robot trajectory X in Figure 4.

$$X^*=\arg\max_X P(X,Z,C)=\arg\min_X-\log P(X,Z,C) \tag{4}$$

Assuming that the prior covariance is Σ, equation (3-4) are brought into equation (2) to obtain the following nonlinear least squares problem:

$$X^*=\arg\max_X\left\{\sum_{r=0}^{R-1}\left(\|p^r-x_0^r\|_\Sigma^2+\sum_{i=1}^{M_r}\|f_i(x_{i-1}^r,u_i^r)-x_i^r\|_{\Lambda_i^r}^2\right)+\sum_{n=1}^{N}\|h_n(x_{j_n}^{r'_n},e_n)-x_{i_n}^{r_n}\|_{\Gamma_n}^2\right\} \tag{5}$$

Where the notation $\|F\|_\Sigma^2=F^T\Sigma^{-1}F$ for the squared Mahalanobis distance $\sum$ with covariance matrix is used.

The iSAM [11] algorithm is proposed to solve this nonlinear least squares problem. Through a series of transformations, linearization of the measurement equations and subsequent collection of all components in one large linear system yields the following standard least squares problem:

$$\theta^*=\arg\min_\theta\|A\theta-b\|^2 \tag{6}$$

Where the vector $\theta\in R^n$ contains the poses of all robot trajectories. The matrix $A\in R^{m\times n}$ is a large but sparse measurement Jacobian with m measurement rows, and $b\in R^m$ is the right-hand side vector. iSAM reduces the least-squares problem to a linear system with unique solutions by QR decomposition of matrix A:

$$R\theta=d \tag{7}$$

2.2. Pose Graphs Fusion

Initialization is a major problem of the approach to multi-robot mapping described so far. If there is no encounter at the beginning of the sequence, then there is a degree of freedom on the second trajectory

and it is necessary to add a prior to fix the second robot trajectory [12]. However, before the first encounter, there's no a prior good initial estimate. Because any choice is likely to conflict with the first encounter once that is added, as shown in Figure 4.

In order to solve the initialization problem, the concept of a conjunction point is introduced. The conjunction point T_r of the robot trajectory *r* represents the offset of the entire trajectory relative to the global coordinate system. Each pose diagram is first held in its own local coordinate system as shown in Figure 4. Poses are transformed to the global frame by $T_r \oplus x_i^r$. The symbol $\oplus$ is used here to represent the transformation when operating in the 2D plane, composing a pose *a* with a transform *t* is defined as

$$p = a \oplus t = \begin{pmatrix} x_a + x_t \cos\theta_a - y_t \sin\theta_a \\ y_a + x_t \sin\theta_a + y_t \cos\theta_a \, x \\ \theta_a + \theta_t \end{pmatrix} \tag{8}$$

As shown in Figure 5, the conjunction points of the two pose graphs are added. The encounter is a global measurement between the two trajectories, but the pose variables for each trajectory are in the robot's own coordinate system. The conjunctions are used to transform the pose of each pose graph into the global coordinate system. The measurement model h is accordingly modified to $h'_n(x_{j_n}^{r'_n}, e_n, T_{r_n}, T_{r'_n})$, the difference *e* between a pose x_i^r from trajectory *r* and a pose $x_j^{r'}$ from another trajectory *r'* is given by $e = (T_r \oplus x_i^r)\,!\,(T_{r'} \oplus x_j^{r'})$.Therefore, the corresponding item in equation (5) is replaced with $\sum_{n=1}^{N} \left\| h'_n(x_{j_n}^{r'_n}, e_n, T_{r_n}, T_{r'_n}) - x_{i_n}^{r_n} \right\|_{\Gamma_n}^2$.

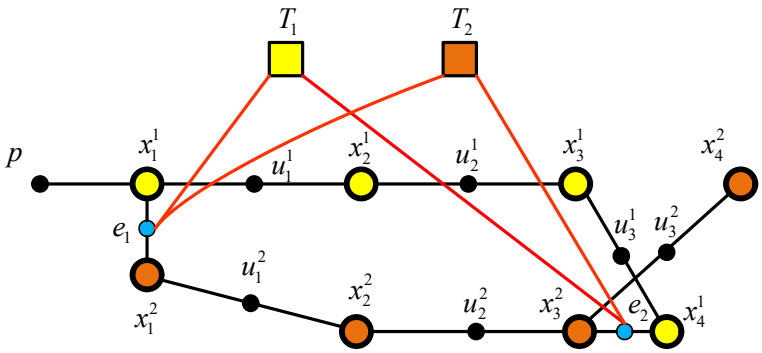

Figure 5. Introduce conjunction points for each trajectory.

Suppose that the robot's loop closing constrain noise term is a zero-mean Gaussian distribution with covariance matrix Θ_{ij}. Adding the loop closing constraint of a single robot, then equation (5) becomes

$$X^* = \arg\max_X \left\{ \sum_{r=1}^{R} \left(\underbrace{\| p^r - x_1^r \|_{\Sigma}^2}_{\text{Prior}} + \underbrace{\sum_{k=1}^{M} \| f_i(x_{i-1}^r, u_i^r) - x_i^r \|_{\Lambda_i^r}^2}_{\text{Sequential frame constraints}} + \underbrace{\sum_{k=1}^{H_r} \left\| f(x_{i_k}^r, u_{i_k j_k}) - x_{jk} \right\|_{\Theta_{ikjk}}^2}_{\text{Loop closing constraints}} \right) \right.$$
$$\left. + \underbrace{\sum_{n=1}^{N} \left\| h'_n(x_{j_n}^{r'_n}, e_n, T_{r_n}, T_{r'_n}) - x_{i_n}^r \right\|_{\Gamma_n}^2}_{\text{Encounter constraints}} \right\} \tag{9}$$

Where p_r represents the number of internal loop closing constraints of robot. An example with three pose graphs is shown in Figure 6. Note that the number of conjunction nodes depends only on the number of robot trajectories.

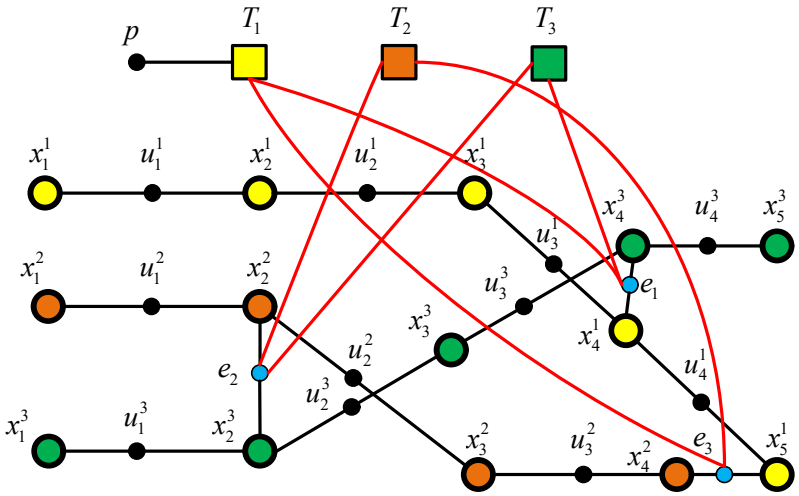

Figure 6. This example shows three encounters between three robots.

3. Experiments and results

This paper carried out two sets of experiments. In the first set of experiments, three robots are used in the indoor environment to verify the effective of the proposed our algorithm. In the second set of experiments, this system was tested by using the famous KITTI data set.

3.1. Indoor Experiment

Three robots equipped with laser performing SLAM on indoor office scenes are shown in Figure 7. These three robots are used to map two different rooms and a corridor in the lab, and the trajectories were represented by red, black and blue. The Figure 8 shows three sub-maps created by above robots. Figure 9 shows a comparison of the global map obtained by performing a direct rigid body transformation with the map obtained by global optimization. Due to the error of the sensor and the noise of each robot's sensor is different, the established map cannot perfectly overlap. However, global optimization using multiple encounter information can avoid accumulated error caused by using the rigid body transformation directly, and the result of mapping is more accurate.

Figure 7. Experiment platform.

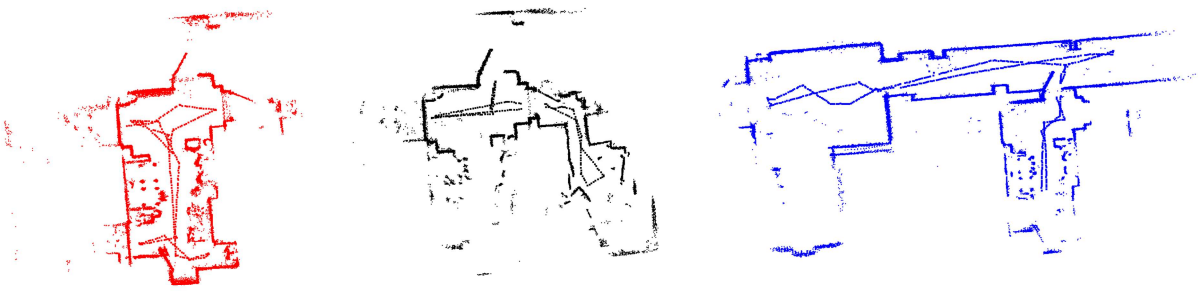

Figure 8. Sub-map from each of the three robots.

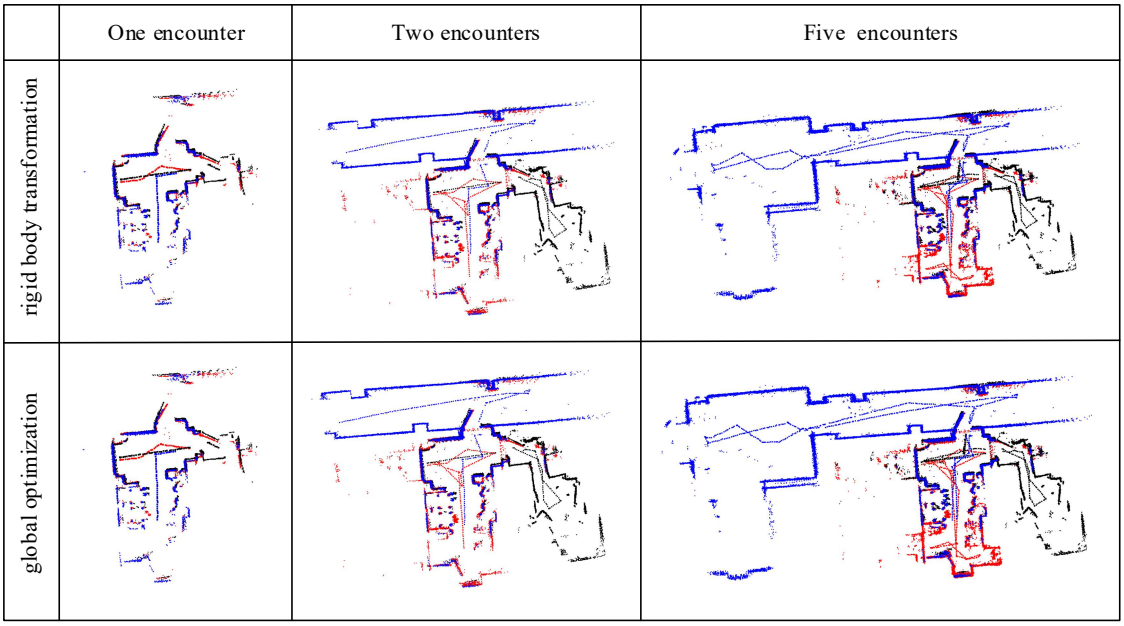

Figure 9. Comparison of the global map obtained by performing a direct rigid body transformation with the map obtained by global optimization.

3.2. KITTI data set

We use the 00 sequence in the famous KITTI dataset, which has a spatial range of 564 meters x 496 meters. We use data from frame 1 to frame 1500 as the first sub-map, and frame 1501 to frame 3000 as the second sub-map, and frame 3001 to frame 4541 as the third sub-map generated from three

robots and the sub-map is shown in Figure 10. Figure 11 shows the perfect fusion of the map. The results show that the algorithm adapts to multiple uncertain encounters between robots and improves the robustness and fault tolerance of SLAM systems.

Figure 10. The sub-map of different areas.

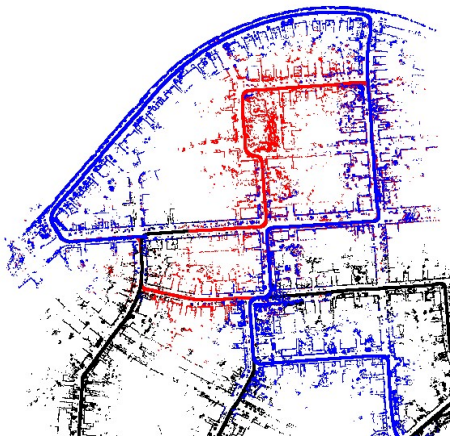

Figure 11. Map fusion results using KIIT data set.

4. Conclusion

Through modeling analysis and experimental verification, the results show that the introduction of conjunction points can avoid the accumulation of errors caused by the direct use of rigid body transformations. At the same time, by introducing the conjunction point, the pose graphs of the robots don't need to be modified when the robots meet each other. The information can be similar to the single robot loop closing transmitting between the two pose graphs, thus solving the problem of multiple encounters of the robot. The fusion of multiple robot pose graphs and the global optimization of the pose map are achieved.

References

[1] S. Saeedi, M. Trentini, M. Seto, and H. Li, "Multiple-robot simultaneous localization and mapping: A review", Journal of Field Robotics, 2016, vol. 33, no.1, pp.3–46.

[2] Cesar Cadena, Luca Carlone, Henry Carrillo, et al. Past, Present, and Future of Simultaneous Localization and Mapping: Toward the Robust-Perception Age [J]. IEEE Transactions on Robotics, 2017, 32(6):1309-1332.

[3] G Reid R, Cann A, Meiklejohn C, et al. Cooperative multi-robot navigation, exploration, mapping and object detection with ROS [J]. 2013, 36(1):1083-1088.

[4] Dong J, Nelson E, Indelman V, et al. Distributed real-time cooperative localization and mapping

using an uncertainty-aware expectation maximization approach [C]// IEEE International Conference on Robotics and Automation. IEEE, 2015:5807-5814.

[5] Rone,W., Ben-Tzvi, P.Mapping, localization and motion planning in mobile multi-robotic systems. Robotica, 2013, 31(1), 1–23.

[6] Kim, B., Kaess, M., Fletcher, L., Leonard, J., Bachrach, A., Roy, N., & Teller, S.Multiple relative pose graphs for robust cooperativemapping. In Proceedings of the IEEE/RSJ International Conference on Robotics and Automation (ICRA), 2010, pp.3185–3192.

[7] Indelman, V., Nelson, E., Michael, N., & Dellaert, F..Multi-robot pose graph localization and data association from unknown initial relative poses via expectation maximization. In International Conference on Robotics and Automation (ICRA), 2014, pp.593–600.

[8] Grisetti G, Kummerle R, Stachniss C, et al. A Tutorial on Graph-Based SLAM[J]. IEEE Intelligent Transportation Systems Magazine, 2011, 2(4):31-43.

[9] Thrun S, Montemerlo M. The Graph SLAM Algorithm with Applications to Large-Scale Mapping of Urban Structures [J]. International Journal of Robotics Research, 2006, 25(5): 403-429.

[10] Gil, A., Reinoso, O., Ballesta, M., & Miguel, J. Multirobot visual SLAM using a Rao-Blackwellized particle filter. Robotics and Autonomous Systems, 2010, 58(1), 68–80.

[11] Kaess M, Ranganathan A, Dellaert F. iSAM: Incremental Smoothing and Mapping [J]. Robotics IEEE Transactions on, 2008, 24(6):1365-1378.

[12] Rone, W., Ben-Tzvi, P.Mapping, localization and motion planning in mobile multi-robotic systems. Robotica, 2013, 31(1), 1–23.